Side Chain Dynamics in Poly(γ-benzyl L-glutamate) as Studied by High-Resolution Solid State ^{13}C Nuclear Magnetic Relaxation in Rotating Frame

Masashi YAMAGUCHI* and Akihiro TSUTSUMI**,†

* Research Institute for Electronic Science, Hokkaido University, Sapporo 060, Japan
** Department of Applied Physics, Faculty of Engineering,
Hokkaido University, Sapporo 060, Japan

ABSTRACT: The rotating frame ^{13}C spin-lattice relaxation time for poly(γ-benzyl L-glutamate) (PBLG) in the solid state was measured by the cross polarization/magic angle spinning (CP/MAS) NMR. From the ^{13}C spin-lock frequency dependence of 'observed' relaxation time $T_{1\rho}^*$, it was revealed that the spin-lattice process with a relaxation time $T_{1\rho}$ is dominant rather than the spin-spin process. Thus, $T_{1\rho}$ measurement gives the information about the dynamical behaviors in PBLG. The temperature dependence of $T_{1\rho}$ was investigated above room temperature. The $T_{1\rho} \sim$ temperature curves for side chain carbons showed a minimum, whose value is much larger than the expected one for the isotropic motion with a single distribution of the correlation time. It was suggested that side chain motion is highly anisotropic and/or the distribution of the correlation time is excessively broad. However, the temperature causing such a $T_{1\rho}$ minimum is very close to that for previously reported β-process corresponding to motion of whole side chain. Further, $T_{1\rho}$ results showed that the motion of benzyl group at the end of side chain contributes dominantly to the β-process. The effect of MAS rate on $T_{1\rho}$ is briefly discussed.
KEY WORDS CP/MAS ^{13}C NMR / Rotating Frame Relaxation / Spin-Locking Frequency / Poly(γ-benzyl L-glutamate) / Side Chain Dynamics /

The physical properties of α-helical poly-(peptide)s in solid state have been investigated extensively from various points of view.[1−3] It has been reported that the side chain of poly(glutamate) undergoes considerable motion above a room temperature. The side chains of some polypeptides show glass-like transition which is similar to the glass transition in amorphous polymers.[4] The temperature dependence of correlation frequency of molecular motion measured by dielectric and mechanical relaxations obeyes the Williams–Landel–Ferry (WLF) equation,[5] which is usually applicable to the main chain motion. This implies the cooperative motion of side chains. Thus, it is of interest to reveals the relation between the local mobility of the side chain and cooperativity of side chain motion.

It is well known that solid state ^{13}C high-resolution NMR is one of the most useful methods for studying local structures and dynamics of polymers. The measurement of ^{13}C relaxation times gives us the information about the local mobility of side chains, which is very different character from ^{1}H relaxation measurement, such as ^{1}H spin-lattice relaxation time in rotating frame, ^{1}H $T_{1\rho}$.[6] It is known that ^{1}H $T_{1\rho}$ is susceptible to the homonuclear spin-diffusion process, which thermally mixes throughout the sample and

only one relaxation time is obtained even if the local mobility of molecule is different in each portion. Further, ^{13}C high resolution NMR has an advantage compared to ^{2}H NMR measurement, which is also useful to study local mobility, since an isotope labeling is not required, which is sometimes very difficult or impossible.

It is well known that $T_{1\rho}$ measurement is sensitive to mid-kHz motion, while T_1 measurement is sensitive to much higher frequency motion (several tens MHz). For the bond rotation in the solid state, the mid-kHz motion seems important. The combination of ^{13}C $T_{1\rho}$ measurement and CP/MAS NMR allows us to observe relatively slow relaxation process (mid-kHz), with high resolution and high sensitivity. From these reasons, ^{13}C $T_{1\rho}$ measurement is potentially the most useful method for studying the polymer motion in the solid state. But, in actual case, the existence of the heteronulear spin-spin process makes the interpretation of ^{13}C $T_{1\rho}$ results complicate. The 'observed' ^{13}C spin-lattice relaxation time in rotating frame, $T_{1\rho}^*$, is not always equal to real $T_{1\rho}$ value. Under a certain condition $T_{1\rho}^*$ even does not reflect molecular motion. For the use of ^{13}C $T_{1\rho}$ to the study of amorphous polymers, it has been reported that the ^{13}C $T_{1\rho}^*$ can be interpreted qualitatively in terms of the molecular motion process.[7,8] In this work, we measured the ^{13}C $T_{1\rho}^*$ of the side chain in α-helical poly-(γ-benzyl L-glutamate) (PBLG) and show that the results are interpreted by molecular motion. Further we discussed the local dynamics of side chains of PBLG.

EXPERIMENTAL

Materials

PBLG was obtained by polymerizing the N-carboxyanhydride (NCA) of γ-benzyl L-glutamate in dioxane at room temperature using triethylamine as an initiator. Sample in the form of film was casted from the
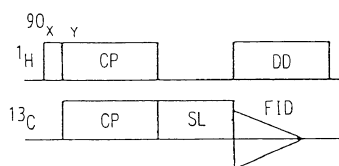

Figure 1. Pulse sequence used for the measurement of ^{13}C $T_{1\rho}$ with CP, where CP, cross polarization; DD, dipole decoupling; FID, free induction decay; SL, spin locking.

chloroform solution at room temperature, and annealed at 130°C for 12 hours. For the NMR measurement, the films were cut to a small pieces before annealing, and were packed randomly in the rotor.

Measurements

^{13}C cross polarization/magic angle spinning (CP/MAS) NMR spectra were measured with Bruker MSL-200 spectrometer (50.3 MHz). MAS rate was about 3.85 kHz, and contact (CP) times were 0.5 to 2 ms. The chemical shift was calibrated through the external adamantane (29.5 ppm relative to tetramethyl-silane, TMS). The pulse sequence used for ^{13}C $T_{1\rho}$ measurement is shown in Figure 1. The spin-lock frequency of ^{13}C spin is varied in the range of 40—73.5 kHz.

The assignment of each peak was made referring to the NMR spectra in solutions. From the chemical shift values of C_α and C (amide), it was confirmed that the main chain takes an α-helical form in the temperature range of this work.[9]

RESULTS AND DISCUSSION

Applicability of $T_{1\rho}^*$ Measurement for the Study of Side Chain Dynamics

Theoretical. In Figure 2, a thermodynamic model for the ^{13}C rotating frame experiment is shown.[6] The ^{13}C rotating frame Zeeman system is coupled to both the lattice system and the proton dipole reservoir with the spin-lattice relaxation time in rotating frame, $T_{1\rho}$, and cross relaxation time, T_{CH}, respectively.
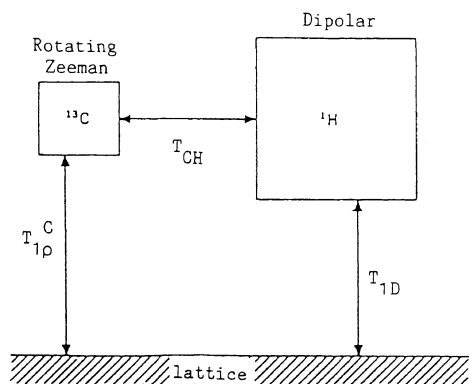
Figure 2. Schematic representation of ^{13}C $T_{1\rho}$ experiment. ^{13}C Rotating Zeeman system is coupled to the lattice with a relaxation time of ^{13}C, $T_{1\rho}$, by molecular motion, and to the ^{1}H dipole system with a relaxation time of the spin-spin fluctuation, T_{CH}. ^{1}H Dipole system is coupled to the lattice with spin-lattice relaxation time of the dipole system, $T_{1\text{D}}$.

At the same time, the proton dipole system is coupled to the lattice system with $T_{1\text{D}}$, which is the spin-lattice relaxation time of the dipolar system. The time development of ^{13}C magnetization is affected by all these processes. Thus, the interpretation of experimental result is quite complicated. However, under a certain condition, some of these processes can be negligible.

It has been reported that the dipole order of ^{1}H system is destroyed quickly by the sample spinning. Garroway reported that when the sample spinning frequency is several kHz, $T_{1\text{D}}$ is expressed as follows depending on the sample spinning frequency.[10]

$$1/T_{1\text{D}} = (\pi/2)3\omega_r^2\tau_{\text{D}}' \qquad (1)$$

where $\tau_{\text{D}}' = (3/M_{\text{HH}}^{(2)})^{1/2}$ is the dipole fluctuation time and $M_{\text{HH}}^{(2)}$ is the Van Vleck proton–proton second moment. ω_r is MAS rate. In the case of PBLG, $M_{\text{HH}}^{(2)}$ is at most 20 Gauss^2 from the results of broad line ^{1}H NMR[11] (less than 10 Gauss^2 above room temperature), and the MAS rate in this experiment is about 3.85 kHz. $T_{1\text{D}}$ is estimated as 25 μs at most (for $M_{\text{HH}}^{(2)} = 20$ Gauss^2) by eq 1. The 'observed' relaxation time, $T_{1\rho}^*$, of PBLG for each carbon

is the order of ms, as will see later, indicating that the inequality, $T_{1\text{D}} \ll T_{\text{CH}}$, $T_{1\rho}$, holds. Thus, in the relaxation process of ^{13}C magnetization, it is considered that the proton dipole system always attains a common spin temperature with the lattice system after the short $T_{1\text{D}}$ value. Therefore, ^{13}C rotating frame magnetization has two possible pass ways to relax, that is, $T_{1\rho}$ process and T_{CH} process. Under these conditions, $T_{1\rho}^*$ is expressed as follows.[6]

$$1/T_{1\rho}^* = 1/T_{1\rho} + 1/T_{\text{CH}} \qquad (2)$$

The former process is concerned to the motional modulation of the spin interaction, whereas the latter process concerned to the mutual flip-flop of heteronuclear spin pairs, which does not need molecular motions. Thus, it is important to know which process is dominant in $T_{1\rho}^*$. To observe T_{CH} directly, the pulse sequence has been proposed by Schaefer et. al.,[7] for which delicate depolarization process is required. But these delicate determination is beyond the scope of this work. The one of more conventional methods to know the dominant process is to see the ^{13}C spin-lock frequency, $\omega_{1\text{C}}$, dependence of $T_{1\rho}^*$, since $T_{1\rho}$ and T_{CH} have a very different $\omega_{1\text{C}}$ dependence.

In a weak collision treatment and under the conditions of ω_{H}, $\omega_{\text{C}} \gg \omega_{1\text{C}}$, where ω_{H} and ω_{C} are the Zeeman frequency of carbon and proton, respectively, $T_{1\rho}$ is expressed as follows.

$$\begin{aligned} 1/T_{1\rho} = (1/3)S(S+1)\{&(2/3)j_{20}(\omega_{1\text{C}}) \\ &+ j_{21}(\omega_{\text{H}}) + (1/6)j_{20}(\omega_{\text{H}} - \omega_{\text{C}}) \\ &+ (1/2)j_{21}(\omega_{\text{C}}) + j_{22}(\omega_{\text{H}} + \omega_{\text{C}})\} \end{aligned} \qquad (3)$$

with

$$j_{kq}(\omega) = \langle \delta A_{kq}^2 \rangle \tau_k / (1 + \omega^2 \tau_k^2)$$

and

$$\delta A_{kq} = A_{kq} - \langle A_{kq} \rangle$$

Where A_{kq} is the rank-2 irreducible spherical tensor which describes spin interactions, $\langle A_{kq} \rangle$

Table I. Contribution from each term in eq 3 around $T_{1\rho\,minimum}(\tau_{min} \sim 1/\omega_{1C})$ assuming isotropic motion of ^{13}C$-^1$H spin pair. Where $\omega_{1C}/2\pi = 73.5$ kHz, $\omega_C/2\pi = 50.3$ MHz, $\omega_H/2\pi = 200.13$ MHz

Term	Value
$j_{20}(\omega_{1C})$	$\sim \tau_{min}/2$
$j_{21}(\omega_H)$	$\sim \tau_{min}/7.4 \times 10^{-6}$
$j_{20}(\omega_H - \omega_C)$	$\sim \tau_{min}/4.2 \times 10^{-6}$
$j_{21}(\omega_C)$	$\sim \tau_{min}/4.6 \times 10^{-5}$
$j_{22}(\omega_H + \omega_C)$	$\sim \tau_{min}/1.3 \times 10^{-7}$

is the value of A_{kq} at equilibrium. The detailed definition of these tensors are seen elsewhere.[12] If isotropic motion of spin-pairs is assumed, correlation time, τ_k does not depend on k, and $\tau_k = \tau_C$, $k = 0, 1, 2$.

The value of each term in eq 3 around the $T_{1\rho}$ minimum is summarized in Table I. Our interest here is the motion of the mid-kHz range. Contribution from the term except first term, which does not contain ω_H or ω_C, is very small and can be negligible. Then, eq 3 is rewrite as follows.

$$1/T_{1\rho} = (1/3)S(S+1)(2/3)j_{20}(\omega_{1C}) \quad (4)$$

Thus, $T_{1\rho}$ has the dependence on ω_{1C} at most quadratic.

T_{CH} can be expressed as $1/T_{CH} = (1/2)M_{CH}^{(2)} \times J_D(\omega_{1C})$,[13,14] where $J_D(\omega_{1C}) = \pi\tau_D\exp(-\omega_{1C}\tau_D)$ and $\tau_D = (9/KM_{HH}^{(2)})^{1/2}$, under the on resonance condition. Where $M_{HH}^{(2)}$ and $M_{CH}^{(2)}$ are second moment of ^{13}C$-^1$H dipolar interaction. K is the geometric factor involving both ^{1}H$-^1$H and ^{13}C$-^1$H dipolar interaction. Thus, T_{CH} has the dependence on ω_{1C} as $\exp(\tau_D\omega_{1C})$.

From these consideration, it is seen that the measurement of spin-lock frequency dependence of $T_{1\rho}^*$ can be used as a criteria whether $T_{1\rho}^*$ reflects molecular motion or not.[6]

Spin-Lock Frequency Dependence of $T_{1\rho}^*$. The experimental results of ω_{1C} dependence of $T_{1\rho}^*$ for PBLG at room temperature are shown in Figure 3 together with the calculated curves proportional to the square of ω_{1C} and
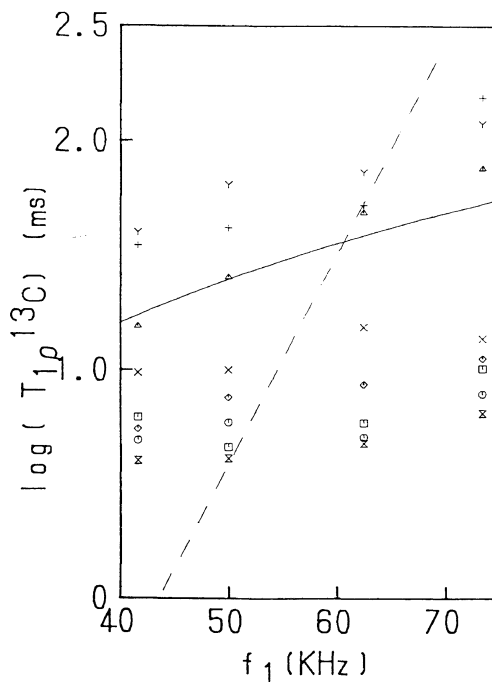

Figure 3. Spin-lock frequency, f_1, dependence of ^{13}C $T_{1\rho}$ for each carbon of PBLG. $\triangle$, C_α; $\diamond$, C_β; $\square$, C_γ; $\bigcirc$, C_{bz}; $+$, CO(ester); Y, CO(amide); X, C_{phe}; $\times$, C'_{phe}. Solid line is proportional to f_1^2 and broken line is proportional to $\exp(\tau_D^2\pi f_1)$, where $\tau_D = 33.6\,\mu s$.

$\exp(\tau_D\omega_{1C})$. The results for all carbons show a dependence similar to square of ω_{1C}, and no exponential dependence on ω_{1C} is observed, indicating $T_{1\rho}$ process is a dominant process in the observed $T_{1\rho}^*$. For C_α, which is in α-helical main chain, $T_{1\rho}^*$ is longer than other carbons except for carbonyl carbons and its frequency dependence is slightly larger than ω_{1C}^2. These results indicate that the contribution from T_{CH} process becomes larger for C_α, because of longer $T_{1\rho}$ value. For other carbons, the frequency dependence of $T_{1\rho}^*$ is smaller than quadratic. At the higher temperature, it is expected that T_{CH} becomes longer because of the partial averaging of spin-spin interaction. Thus, it is expected that $T_{1\rho}$ process is dominant in $T_{1\rho}^*$ as far as $T_{1\rho}$ is shorter than that at room temperature. These results indicate that the observed ^{13}C $T_{1\rho}$ can
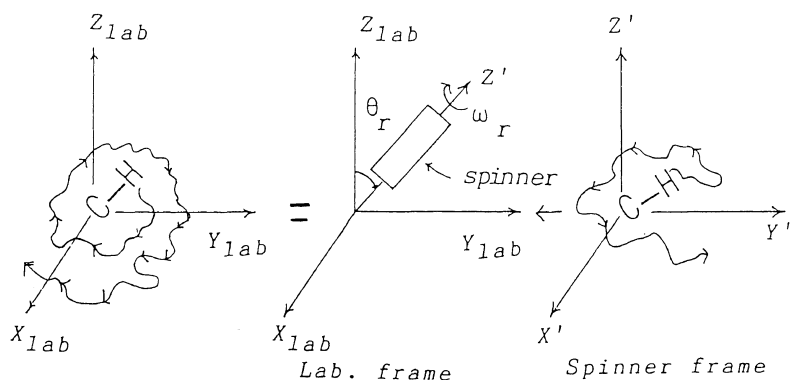
Figure 4. Coordinate transformation for MAS experiments. The direction of ^{13}C–^{1}H spin pair in the laboratory frame changes by both molecular motion and sample spinning. These two contributions are decomposed by the transformation from spinner to the laboratory frame in which sample spinning effects are included.

be discussed in terms of the molecular motion for PBLG. Hereafter, we neglect second term in eq 3, and put $T_{1\rho}^{*} = T_{1\rho}$.

The Influence of Sample Spinning on ^{13}C $T_{1\rho}$

All ^{13}C $T_{1\rho}$ experiments are performed under MAS condition. Before discussing about the $T_{1\rho}$ results more precisely, it is important to see the effects of MAS rate on $T_{1\rho}$ value. Haeberlen and Waugh discussed the effect of sample spinning on $T_{1\rho}$ in weak collision limit in the case of homonuclear dipole interaction.[16] In the case of heteronuclear dipole interaction, the spectral density in eq 4 is replaced with

$$j_{20}(\omega_{1C}) = \langle \delta A_{20}^2 \rangle \sum | d_{q,0}^{(2)}(\theta_r) |^2 \tau_C /$$
$$\{1 + (\omega_{1C} + q\omega_r)^2 \tau^2\} \tag{5}$$

where $d_{q,0}^{(2)}(\theta_r)$ is reduced Wigner rotation matrix which describes the transformation from the laboratory frame, whose Z-axis is parallel to the static field, to the rotor frame (rotating with an angular frequency ω_r about the axis which is tilted with a magic angle θ_r to the static field). (see Figure 4) Detailed derivation of eq 5 is shown in Appendix. Substituting eq 5 into 4 assuming the isotropic motion and magic angle condition, $\theta_r = 54.7°$
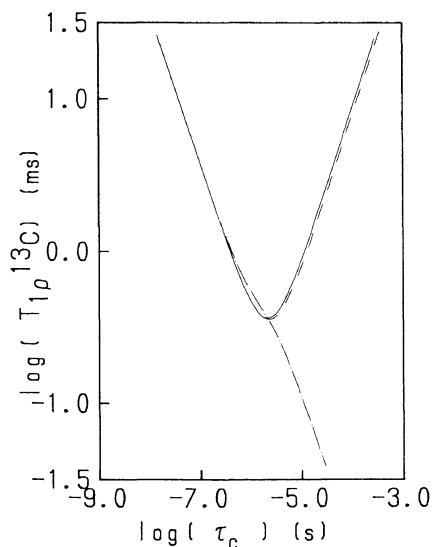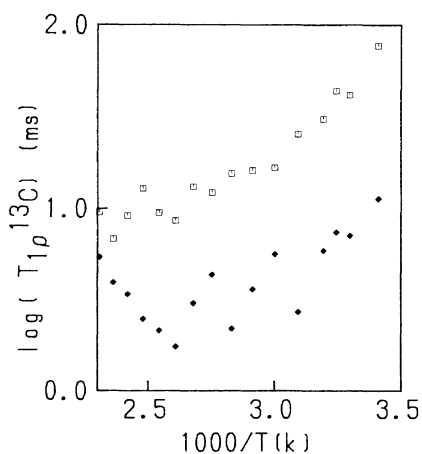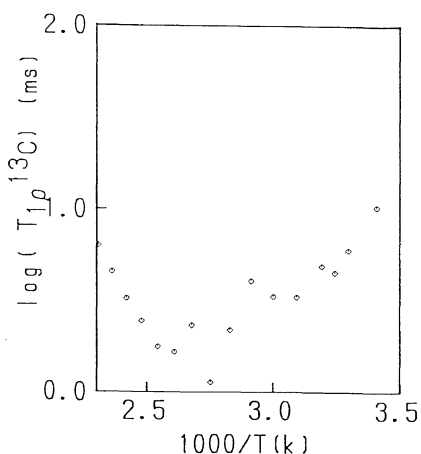

Figure 5. τ_C dependence of ^{13}C $T_{1\rho}$ calculated using eq 6 under the conditions of $f_1 = 73.5\,\mathrm{kHz}$ and ———, $f_r = 0\,\mathrm{Hz}$; ———, $f_r = 10\,\mathrm{kHz}$; ———, $f_r = 73.5\,\mathrm{kHz}$ where f_r is the MAS rate.

$$1/T_{1\rho} = (1/40)(\gamma_H^2 \gamma_C^2 \hbar^2 / r^6)$$
$$\cdot (3 \sin^4 \theta_r \tau_C / (1 + (\omega_{1C} + 2\omega_r)^2 \tau_C^2))$$
$$+ 12 \sin^2 \theta_r \cos^2 \theta_r \tau_C / (1 + (\omega_{1C} + \omega_r)^2 \tau_C^2)$$
$$+ 12 \sin^2 \theta_r \cos^2 \theta_r \tau_C / (1 + (\omega_{1C} - \omega_r)^2 \tau_C^2)$$
$$+ 3 \sin^4 \theta_r \tau_C / (1 + (\omega_{1C} - 2\omega_r)^2 \tau_C^2) \tag{6}$$

The dependence of $T_{1\rho}$ on τ_C with various MAS

(a)

(b)

Figure 6. Temperature dependence of ^{13}C $T_{1\rho}$ for C_α (□) and C_β (◆) (a) and C_γ (◇) (b) of PBLG. Spin-lock frequency $f_1 = 73.5\,\text{kHz}$ and MAS rate $f_r = 3.85\,\text{kHz}$.

Figure 7. Temperature dependence of ^{13}C $T_{1\rho}$ for C_{bz} (□) and C_{phe} (◆) of PBLG. Spin-lock frequency $f_1 = 73.5\,\text{kHz}$ and MAS rate $f_r = 3.85\,\text{kHz}$.

Table II. ^{13}C $T_{1\rho\,\text{minimum}}$ for each carbon (PBLG)

	Experiment	Calculation
C_β	1.53 (ms)	0.11 (ms)
C_γ	1.15	0.11
C_{bz}	1.15	0.11
C_{phe}	1.55	0.22

rates is shown in Figure 5. The effect of MAS rate is seen in the region of $(\omega_{1C} + q\omega_r)\tau_C > 1$. $T_{1\rho}$ minimum occurs at slightly longer τ_C region and becomes smaller as increasing MAS rate. In the case of $\omega_{1C} = \omega_r$, the $T_{1\rho}$ minimum is not observed since $j_{20}(\omega_{1C})$ contains the term proportional to τ_C as in the case of T_2 without sample spinning.[16] Under the condition of this work, $\omega_r/2\pi = 3.85\,\text{kHz}$, the effect of MAS can be negligible.
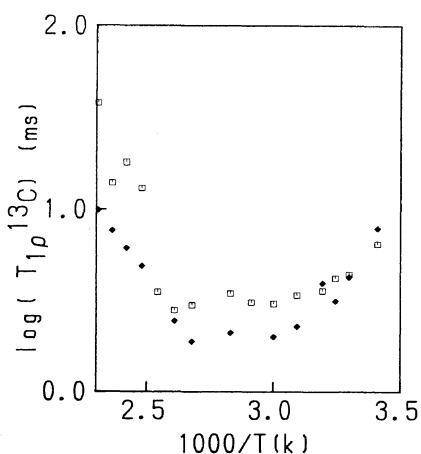
Temperature Dependence of ^{13}C $T_{1\rho}$

The temperature dependence of ^{13}C $T_{1\rho}$ with a spin-lock power of 73.5 kHz for each carbon of PBLG is plotted in Figures 6 and 7. A scattering of the data points may partly come from the overlap of the peaks. For carbons in the side chain, a $T_{1\rho}$ minimum is observed, where τ_C has a value of $1/\omega_{1C}$. Whereas $T_{1\rho}$ of the main chain carbon, C_α, does not show the $T_{1\rho}$ minimum and decreases with increasing temperature, indicating that τ_C is in the region longer than $1/\omega_{1C}$ and the main chain motion is slower than the side chain motion.

$T_{1\rho}$ minimum value for each carbon is summarized in Table II with calculated ones, in which the contributions of proton dipolar interactions only from the nearest neighbor are taken into account. $T_{1\rho}$ takes its minimum value around $\omega_{1C}\tau_C = 1$. From eq 4 with

assuming isotropic motion of ^{1}H–^{13}C pairs, that is, $j_{20} = \langle \delta A_{20}^2 \rangle \tau/(1 + \omega^2 \tau^2)$, $T_{1\rho}$ minimum value is given by

$$T_{1\rho\,\text{minimum}} = 12\omega_{1\text{C}}/\langle \delta A_{20}^2 \rangle \qquad (7)$$

$$\langle \delta A_{20}^2 \rangle = (6/5)\gamma_{\text{C}}^2 \gamma_{\text{H}}^2 \hbar^4/r^6,$$

where γ_{C} and γ_{H} are gyromagnetic ratio of ^{13}C and ^{1}H nuclei, respectively. r is the distance between ^{13}C and ^{1}H nuclei, $r = 1.09$ A.[17]

The experimental values are almost one order smaller than calculated ones for all carbons. In the solid state, the contributions from other protons, such as the second nearest neighbor, 3rd nearest neighbor and so on, are important. If these contributions are considered, the calculated values becomes furthermore smaller and the disagreement between experimental and calculated values becomes larger. These results can not be explained by isotropic motion model with single correlation

Figure 8. Relaxation map for β-process of PBLG. f_{C} is characteristic frequency. In ^{13}C $T_{1\rho}$ experiment, results obtained at spin-lock frequency $f_1 = 73.5$ kHz and MAS rate $f_r = 3.85$ kHz are shown. ⊙, ◇, △, dielectric; □, mechanical.

time, and may indicate that the distribution of correlation time is quite broad and/or the side chain motion is highly anisotropic. (In both cases, minimum value of relaxation time becomes larger than isotropic motion case.[19])

To see the relation between the results of $T_{1\rho}$ experiments and other methods such as the mechanical and dielectric relaxation experiments,[20] the correlation frequency, f_{C}, which is defined as $f_{\text{C}} = 1/(2\pi\tau_{\text{C}})$, is plotted against the reciprocal of the absolute temperature in Figure 8. It is expected that if $T_{1\rho}$ experiment and other experiments reflect the same motional process, τ_{C} of $T_{1\rho}$ takes the similar value to other experiments. Especially, in $T_{1\rho}$ experiment, it is expected to show which part of molecule is mainly contributed to the motional process. The plots for the mechanical and dielectric relaxations are corresponding to the process for the large scale side chain motion of PBLG (β-process).[4] It has been reported that these curve shows WLF type temperature dependence.[4] The results of $T_{1\rho}$ for side chain carbons are located close to the curve for other relaxation experiments. Although the $T_{1\rho}$ minimum for C_α in α-helical main chain is far from such curve. These results indicate that the motional process reflected in $T_{1\rho}$ for side chains are corresponding to β-process. Further, f_{C} positions for side chains approach the more to the curve as remote from the main chain.

These results implies that β-process is mainly caused by the side chain portion which is remote from the main chain.

CONCLUSION

It was found that the spin-lattice process rather than the spin-spin process is dominant in ^{13}C $T_{1\rho}$ for side chain carbons of α-helical PBLG, and the information about molecular motion is directly obtained. The comparison of the temperature position of the $T_{1\rho}$ minimum to other relaxation experiments showed that the motional process reflected in $T_{1\rho}$ is
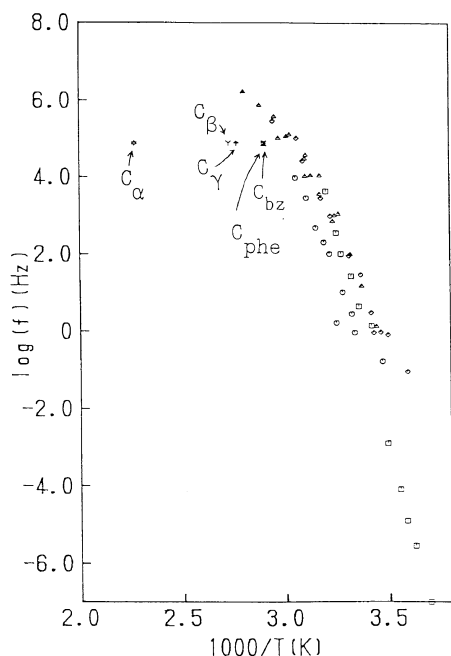
mainly corresponding to β-process. Further, use of the high-resolution NMR suggests that the motion of the portion remote from the main chain is dominant in β-process.

APPENDIX

Hamiltonian of heteronuclear dipole interaction is given in spherical tensor representation as follows.

$$H_D = \sum (-1)^q A_{2,q}^L(t) T_{2,-q} \qquad \text{(A-1)}$$

where $A_{2,q}^L(t)$ and $T_{2,-q}$ are spherical tensors which represent the lattice function and the spin operator, respectively. Difinitions of these tensors are seen elsewhere.[12] Superscript 'L' indicates that $A_{2,q}^L(t)$ is defined in the laboratory frame.

Sample is spinning about the axis tilted angle θ_r to the Zeeman field with the rate $\omega_r = 2\pi f_r$ (rad s^{-1}) as shown in Figure 4. $A_{2,q}^L(t)$ is expressed by $A_{2,q}(t)$, which is lattice function defined in spinner frame (see Figure 4) as follows.

$$A_{2,0}^L(t) = \sum A_{2,q}(t) \exp(-iq\omega_r t) d_{q,0}^{(2)}(\theta_r) \quad \text{(A-2)}$$

Where $d_{q,0}^{(2)}(\theta_r)$ is the reduced rotation matrix. Note, $A_{2,0}^L(t)$ has dependence on the time caused from both of the sample spinning and molecular motion, whereas $A_{2,q}(t)$ depends on the time caused from only molecular motion.

The correlation time of $A_{2,0}^L(t)$ and corresponding spectral density are expressed as follows.

$$
\begin{aligned}
&\langle \delta A_{2,0}^L(0) \delta A_{2,0}^L(t) \rangle \\
&= \sum |d_{q,0}^{(2)}(\theta_r)|^2 \\
&\quad \cdot \langle \delta A_{2,-q}(0) \delta A_{2,q}(t) \rangle \exp(-i\omega_r t)
\end{aligned}
\qquad \text{(A-3)}
$$

$$
\begin{aligned}
j_{2,0}(\omega_{1C}) &= \sum |d_{q,0}^{(2)}(\theta_r)|^2 \\
&\quad \cdot \mathrm{Re} \int \langle \delta A_{2,-q}(0) \delta A_{2,q}(t) \rangle \\
&\quad \cdot \exp\{-i(\omega_{1C} + q\omega_r)t\} \mathrm{d}t
\end{aligned}
\qquad \text{(A-4)}
$$

In the case of the powder sample undergoing

isotropic molecular motion,

$$\langle \delta A_{2,-q}(0) \delta A_{2,q}(t) \rangle = \langle \delta A_{2,q}^2 \rangle \exp(-t/\tau_C) \qquad \text{(A-5)}$$

and

$$\langle \delta A_{2,q}^2 \rangle = \langle A_{2,0}^2 \rangle \qquad \text{(A-6)}$$

Substituting (A-5, 6) into (A-4) and performing integration give

$$
j_{2,0}(\omega_{1C}) = \langle A_{2,0}^2 \rangle \sum |d_{q,0}^{(2)}(\theta_r)|^2 \tau_C / \\
\{1 + (\omega_{1C} + q\omega_r)^2 \tau_C^2\} \qquad \text{(A-7)}
$$

REFERENCES

1. M. Tsuboi, *J. Polym. Sci.*, **59**, 139 (1962).
2. J. Watanabe and I. Uematsu, *Polymer*, **25**, 1711 (1984).
3. A. Tsutsumi, K. Hikichi, and M. Kaneko, *Polym. J.*, **10**, 437 (1978).
4. A. Tsutsumi, K. Hikichi, T. Takahashi, Y. Yamashita, M. Matsushima, M. Kanke, and M. Kaneko, *J. Macromol. Sci., Phys.*, **B8**, 413 (1973).
5. J. Ferry, "Viscoelastic Properties of Polymers," John Wiley and Sons Inc., New York, N.Y., 1962.
6. D. L. VanderHart and A. N. Garroway, *J. Chem. Phys.*, **71**, 2773 (1979).
7. J. Schaefer, E. O. Stejskal, T. R. Steger, M. D. Sefcik, and R. A. Mckay, *Macromolecules*, **13**, 1121 (1980).
8. J. Schaefer, E. O. Stejskal, and R. Buchdahl, *Macromolecules*, **10**, 384 (1977).
9. A. Shoji, T. Ozaki, H. Saito, R. Tabeta, and I. Ando, *Macromolecules*, **17**, 1472 (1984).
10. A. N. Garroway, *J. Magn. Reson.*, **34**, 263 (1979).
11. A. Tsutsumi, S. Anzai, and K. Hikichi, *Polym. J.*, **15**, 355 (1983).
12. M. Mehring, "Principles of High Resolution NMR in Solids," Springer-Verlag, Berlin, 1983.
13. D. E. Demco, J. Tegenfeld, and J. S. Waugh, *Phys. Rev.*, **11**, 4113 (1975).
14. K. Akasaka, S. Ganapathy, C. A. McDowell, and A. Naito, *J. Chem. Phys.*, **78**, 3567 (1983).
15. T. T. P. Ceung and R. Yaris, *J. Chem. Phys.*, **72**,

3604 (1980).

16. U. Haeberlen and J. S. Waugh, *Phys. Rev.*, **185**, 420 (1969).

17. P. J. Flory, "Statistical Mechanics of Chain Molecules," Interscience, New York, N.Y., 1969.

18. V. J. McBriety, *Polymer*, **15**, 503 (1974).

19. G. Lipari and A. Szabo, *J. Chem. Phys.*, **104**, 4559 (1982).

20. Y. Yamashita, A. Tsutsumi, K. Hikichi, and M. Kaneko, *Polym. J.*, **8**, 114 (1975).